Molecular Biology of the Cell
Vol. 15, 2684–2696, June 2004

Endocytic Trafficking Routes of Wild Type and ΔF508 Cystic Fibrosis Transmembrane Conductance Regulator[D]

Martina Gentzsch,* Xiu-Bao Chang,* Liying Cui,* Yufeng Wu,* Victor V. Ozols,* Amit Choudhury,† Richard E. Pagano,† and John R. Riordan*‡

*Mayo Clinic College of Medicine, S.C. Johnson Medical Research Center, Department of Biochemistry and Molecular Biology, Mayo Clinic, Scottsdale, Arizona 85259; and †Mayo Clinic College of Medicine, Department of Biochemistry and Molecular Biology and Thoracic Diseases Research Unit, Mayo Clinic, Rochester, Minnesota 55905

Submitted March 3, 2004; Revised March 29, 2004; Accepted March 29, 2004
Monitoring Editor: Vivek Malhotra

Intracellular trafficking of cystic fibrosis transmembrane conductance regulator (CFTR) is a focus of attention because it is defective in most patients with cystic fibrosis. ΔF508 CFTR, which does not mature conformationally, normally does not exit the endoplasmic reticulum, but if induced to do so at reduced temperature is short-lived at the surface. We used external epitope-tagged constructs to elucidate the itinerary and kinetics of wild type and ΔF508 CFTR in the endocytic pathway and visualized movement of CFTR from the surface to intracellular compartments. Modulation of different endocytic steps with low temperature (16°C) block, protease inhibitors, and overexpression of wild type and mutant Rab GTPases revealed that surface CFTR enters several different routes, including a Rab5-dependent initial step to early endosomes, then either Rab11-dependent recycling back to the surface or Rab7-regulated movement to late endosomes or alternatively Rab9-mediated transit to the *trans*-Golgi network. Without any of these modulations ΔF508 CFTR rapidly disappears from and does not return to the cell surface, confirming that its altered structure is detected in the distal as well as proximal secretory pathway. Importantly, however, the mutant protein can be rescued at the plasma membrane by Rab11 overexpression, proteasome inhibitors, or inhibition of Rab5-dependent endocytosis.

INTRODUCTION

The cystic fibrosis transmembrane conductance regulator (CFTR) is a cell surface glycoprotein that functions as a chloride channel at the apical surface of many epithelial cells (Hanrahan *et al*., 2003). The biosynthetic processing and intracellular trafficking of CFTR have been extensively studied because the most common cystic fibrosis-causing mutation in the CFTR gene (ΔF508) results in a protein that fails to mature conformationally and does not transit from the endoplasmic reticulum to the cell surface (Gelman and Kopito, 2002). This mutation is temperature sensitive (Denning *et al*., 1992), and some degree of maturation and transport to the plasma membrane occurs in cells grown at reduced temperature (Kopito, 1999) or in the presence of certain chemicals (Brown *et al*., 1997). Both wild type and the mutant protein that have reached the surface under these conditions are endocytosed, the later much more rapidly than the former (Heda *et al*., 2001; Sharma *et al*., 2001). Therefore, it has been suggested that the ΔF508 CFTR protein is recognized as aberrant not only by the quality control system of the endoplasmic reticulum (ER) but also in the endocytic pathway (Sharma *et al*., 2001). However, the precise step and molecular basis of this differential recognition of the wild-type and mutant molecules in the endocytic pathway are not known. Several aspects of the internalization of the wild-type CFTR have been elucidated. It has been shown that CFTR is endocytosed by clathrin-coated vesicles (Lukacs *et al*., 1997; Bradbury *et al*., 1999) and a tyrosine-based motif as well as a dileucine sequence in the cytoplasmic C terminus are important for this process (Hu *et al*., 2001; Weixel and Bradbury, 2001). The tyrosine-based motif is recognized by the μ2 subunit of the AP2 adaptor complex and blocking of this interaction prevents endocytosis of wild type CFTR (Weixel and Bradbury, 2001). Recent studies have shown that some of it is recycled after internalization (Picciano *et al*., 2003). Overexpression of a dominant negative form of the Rme-1 protein, which is required for release from recycling endosomes back to the plasma membrane, reduced the amount of cell surface CFTR after endocytosis. This apparent trapping in recycling endosomes was mediated by se-

Article published online ahead of print. Mol. Biol. Cell 10.1091/mbc.E04–03–0176. Article and publication date are available at www.molbiolcell.org/cgi/doi/10.1091/mbc.E04–03–0176.

[D] Online version of this article contains supporting material. Online version is available at www.molbiolcell.org.

‡ Corresponding author. E-mail address: riordan@mayo.edu.

Abbreviations used: CFTR, cystic fibrosis transmembrane conductance regulator; DN, dominant-negative; DsRed, red fluorescent protein; EGFP, enhanced green fluorescent protein; EEA1, early endosomal antigen 1; Extope-CFTR, external-epitope tagged CFTR; EL, extracytoplasmic loop; PDZ, PSD-95/discs large/ZO-1; TGN *trans*-Golgi network; UIM, ubiquitin-interacting motif.

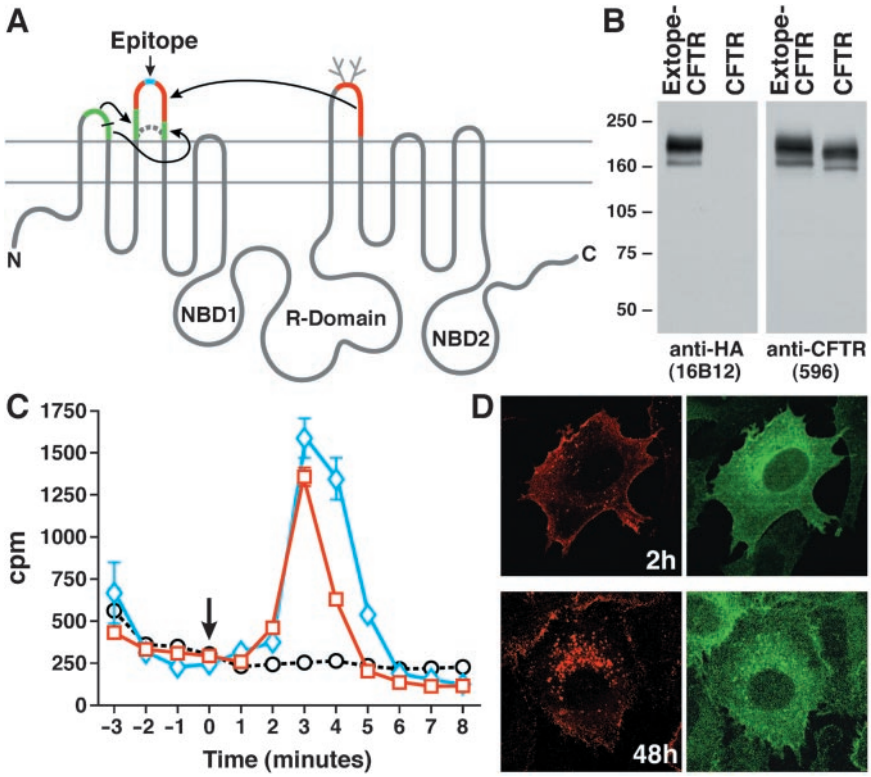

Figure 1. External-epitope tagged CFTR (Extope-CFTR) matures and functions like unmodified wild type CFTR. (A) Schematic of strategy used to generate Extope-CFTR. Portions of EL1 and EL4 sequences incorporated into EL2 flanking a single HA-epitope (blue) are shown in green and red, respectively. (B) Western blot of external-epitope tagged CFTR (Extope-CFTR). Extope-CFTR matures like the unmodified wild type protein. Total cell lysates (25 μg) were separated by 6% SDS-PAGE, transferred to nitrocellulose, and Extope-CFTR was detected with monoclonal mouse anti-HA antibody 16B12 or monoclonal mouse anti-CFTR antibody 596. (C) cAMP stimulated $^{36}Cl^-$ efflux. Extope-CFTR functions as a chloride channel like the unmodified wild type protein. BHK-21 cells stably expressing wild type CFTR (blue diamonds) or Extope-CFTR (red squares) were loaded with $Na^{36}Cl$, transferred to chloride-free buffer, and cAMP-dependent chloride efflux was stimulated with stimulation cocktail as described in MATERIALS AND METHODS. An arrow indicates the stimulation at time 0. Extope-CFTR–expressing cells, which were not stimulated, are shown as control (black circles). Each point represents the average of three independent samples and standard deviations are indicated. (D) Immunofluorescence detection of total and cell surface derived CFTR. Extope-CFTR was labeled on the cell surface with monoclonal mouse anti-HA antibody and cells were reincubated for 2 or 48 h. Cells were fixed, permeabilized, and internalized pools of Extope-CFTR were detected with Alexa Fluor 568 conjugated to goat anti-mouse Fab fragments (left). Total pools of Extope-CFTR were subsequently labeled with anti-CFTR antibody 570 directly conjugated to Alexa Fluor 488 (right).

quence information near the C terminus of CFTR. Another study reported that the PDZ (PSD-95/discs large/ZO-1) protein-binding extreme C terminus of CFTR is involved in endocytic recycling (Swiatecka-Urban *et al.*, 2002). All of the studies of CFTR endocytosis reported to date have relied on labeling of the CFTR molecules at the cell surface using impermeant biotinylation reagents. The kinetic fate of this pool after cell lysis was then followed by pull-down with immobilized streptavidin and detection by immunoblotting or of metabolically incorporated radioactivity in pulse-chase formats. These techniques do not permit direct visualization of the cell surface pool as distinct from the entire CFTR pool in cells because all antibodies to CFTR of sufficient sensitivity recognize cytoplasmic epitopes requiring cell permeabilization for detection. Insertion of exogenous epitopes into extracytoplasmic loops of CFTR is an obvious strategy to overcome this limitation, but this has proven challenging because even minor changes in CFTR sequence tend to compromise its folding to a native state (Riordan, 1999). Howard *et al.* (1995, 2000) inserted a FLAG epitope into the fourth extracellular loop, but this modification removed the sites of attachment of N-linked oligosaccharide chains and the protein was no longer glycosylated. After several attempts at alternative strategies, we have succeeded in inserting a hemagglutinin (HA) epitope into an expanded second extracytoplasmic loop without compromising conformational maturation, glycosylation, or function of CFTR after transient or stable expression in mammalian cells. This has enabled the direct observation by confocal immunofluorescence microscopy and quantitative chemiluminescence of the surface pool as distinct from the total cellular CFTR pool and the ability to follow its movement over time. The movements and their perturbation by various Rab GTPases that regulate different steps in the endocytic pathway show that CFTR enters several different routes including a degradative path to lysosomes, recycling to the plasma membrane and a retrieval route from late endosomes to the *trans*-Golgi network (TGN).

ΔF508 CFTR favors the degradative pathway and is less stable at the plasma membrane than wild type CFTR. Inhibitors of both the proteasome and lysosomal proteases drastically slowed endocytic processing of ΔF508 CFTR, stabilizing the mutant protein at the cell surface or intracellularly, respectively. Furthermore either inhibition of Rab5-dependent internalization or augmentation of a Rab11-dependent recycling step resulted in increased plasma membrane pools of ΔF508. This shows that the mutant protein is capable of being recycled and that shifting the equilibria between different routings in the endocytic pathway can increase the amount at the plasma membrane.

MATERIALS AND METHODS

Construction and Expression of Extope-CFTR

On the basis of earlier modifications of the extracytoplasmic loops of CFTR to insert glycosylation sites at different locations (Chang *et al.*, 1994) and to introduce disease-associated mutations (Hämmerle *et al.*, 2001), we attempted to insert readily detectable epitopes. Most success was achieved by insertion of a single HA epitope in the center of an expanded extracytoplasmic loop (EL)2, which incorporated portions of the longer EL1 and EL4 sequences to become approximately the same length as EL4 (Figure 1A). Details of this construct will be described elsewhere. Stable cell lines expressing this construct with and without phe508 were established.

Cell Culture and Transfection

Baby hamster kidney (BHK-21) cells were obtained from the American Type Culture Collection (Manassas, VA) and grown at 37°C in 5% CO_2. BHK-21 cells stably expressing Extope-CFTR were created by cotransfection of pcDNA3 containing Extope-CFTR and pNUT vector (Chang *et al*., 1993) by using calcium phosphate with subsequent selection with 500 μM methotrexate in the growth medium. Individual clones were isolated and tested for expression by Western blotting. Cells were transiently transfected with pEGFP-Endo (BD Biosciences Clontech, Palo Alto, CA) to express RhoB. Wild-type and dominant negative Rab proteins were expressed transiently as either DsRed fusions by using pDsRed1-C1 (Rab7 and Rab7T22N, Rab9 and Rab9S21N, and Rab11 and Rab11S25N) or pDsRed-C2 (Rab5 and Rab5aN133I) or as fusions to enhanced green fluorescent protein (EGFP) by using pEGFP-C2 (Rab4 and Rab4aN121I). The construction of the Rab expression plasmids has been described recently (Choudhury *et al*., 2002; Sharma *et al*., 2003). For transient transfections, LipofectAMINE Plus Reagent (Invitrogen) was used according to the manufacturer's instructions.

To allow maturation of the mutant protein, BHK-21 cells expressing Extope-ΔF508 CFTR were grown at 27°C for 2 d in the presence of 2 mM butyrate. For comparison, BHK-21 cells expressing Extope-CFTR were grown under the same conditions.

Western Blotting

Cells were washed in ice-cold phosphate-buffered saline (PBS) and lysed with NP-40 lysis buffer (1% NP-40, 150 mM NaCl, 50 mM Tris, pH 7.4, 10 mM $NaMoO_4$) at 4°C for 30 min. Protease inhibitors were added to NP-40 lysis buffer to a final concentration of 1 μg/ml leupeptin, 2 μg/ml aprotinin, 50 μg/ml Pefabloc, 121 μg/ml benzamidine, 3.5 μg/ml E64. Cell lysates were centrifuged at maximal speed in an eppifuge at 4°C, and supernatants were collected. Cell lysates (25 μg) were loaded, separated on 6% SDS-PAGE minigels, and transferred to nitrocellulose. Blots were probed with anti-HA antibody (16B12, 1:1000; Babco, Richmond, CA) or anti-CFTR antibody 596 (1:2000).

Chloride Efflux Assays

The assay was performed as described previously (Chang *et al*., 1999). Cells grown in six-well culture dishes were washed twice with Efflux buffer [136 mM $NaNO_3$, 3 mM KNO_3, 2 mM $Ca(NO_3)_2$, 2 mM $Mg(NO_3)_2$, 10 mM glucose, and 20 mM HEPES, pH 7.4] and loaded with ^{36}Cl by incubation for 1 h with 0.5 ml of Efflux buffer containing 1 μCi of $Na^{36}Cl$ (Amersham Biosciences, Piscataway, NJ). Wells were then washed and samples collected at 1-min intervals after stimulation at time 0 by adding Efflux buffer containing 1× stimulation cocktail (1 mM 3-isobutyl-1-methylxanthine, 10 μM forskolin, 100 μM dibutyryl cyclic AMP). Samples (0.5 ml) were collected into 24-well TopCount plates (PerkinElmer Life and Analytical Sciences, Boston, MA). Microscint 40 (1 ml) was added for scintillation counting.

Confocal Immunofluorescence

Antibody 16B12 was generally used to visualize cell surface and intracellular Extope-CFTR. Fab fragments derived from 16B12 IgGs were produced by the Mayo Clinic Scottsdale Immunology Core Facility by using immobilized Papain (Pierce Chemical, Rockford, IL) according to the instructions of the manufacturer. Subsequently, Fab fragments were separated from undigested IgGs and Fc fragments by using a HiTrap Protein A HP column (Amersham Biosciences) and the purity and integrity of the Fab preparation was confirmed by SDS-PAGE. The staining pattern of Extope-CFTR by using 16B12 IgGs or Fab fragments were similar, when detected by goat anti-mouse Fab (Jackson ImmunoResearch Laboratories, West Grove, PA), followed by donkey anti-goat Alexa Fluor 488 conjugate (Molecular Probes, Eugene, OR) as shown in Supplemental Figure 1A. Because the staining with Fab was however much weaker than with IgG (Supplemental Figure 1B) when routinely detected with polyclonal goat anti-mouse IgG Alexa Fluor 488 conjugate, we used 16B12 IgGs in all further experiments.

16B12 anti-HA antibody binds to Extope-CFTR even at pH 3 to 4 and was therefore not useful for studies were the antibody had to be removed from the epitope. In contrast, anti-HA antibody 12CA5 can be removed from cell surface Extope-CFTR by an acidic wash (2× 30 s in cold PBS, pH 3.7) as shown in Supplemental Figure 2 and was therefore used in studies intended to monitor exclusively internalized intracellular Extope-CFTR.

BHK-21 cells were grown on collagen-coated chamber slides (BD Biosciences, San Jose, CA). For labeling of Extope-CFTR at the surface of intact cells, cells were washed three times with PBS and either precooled for 10 min on ice, followed by labeling of cell surface Extope-CFTR for 30 min on ice with anti-HA monoclonal antibodies (mAbs) (16B12 raw ascites fluid 1: 500, 16B12 Fab 10 μg/ml or 12CA5 protein G purified 5 μg/ml) in PBS with 1% bovine serum albumin (BSA) or alternatively 10 min in regular growth media. Cells were then washed four times with ice-cold PBS, warm growth media was added, and cells were reincubated at 37°C in the incubator for indicated times. To remove 12CA5 mAb bound to cell surface pools of Extope-CFTR, cells were washed twice for 30s with ice-cold PBS pH 3.7, followed by a wash with regular PBS pH 7.4. Cells were fixed in 4% paraformaldehyde for 10 min, washed with PBS, permeabilized in 0.1% saponin in PBS, and blocked with 1% BSA and 5% normal goat serum in PBS. Secondary antibodies were goat anti-mouse Fab fragments or IgGs conjugated to Alexa Fluor 488, 568, or 633. Anti-early endosome antigen 1 (EEA1) antibody was directly labeled with fluorescein isothiocyanate (BD Transduction Laboratories). Rabbit anti γ-Adaptin antibody was from Santa Cruz Biotechnology (Santa Cruz, CA). The mouse mAb 596 recognizes an epitope in nucleotide binding domain 2 of CFTR. Rho B was expressed as a green fluorescent protein (GFP) fusion by using pEGFP-Endo (BD Biosciences Clontech). Wild-type and dominant negative Rab proteins were expressed as either as DsRed fusions (Rab5 and Rab5aN133I, Rab7 and Rab7T22N, Rab9 and Rab9S21N, Rab11 and Rab11S25N) or as fusions to EGFP (Rab4a and Rab4aN121I). Lysosomes were stained with Lysotracker Red (Molecular Probes) for 1 h according to the instructions of the manufacturer. Dextran Alexa Fluor 568 (10,000 Da), transferrin Alexa Fluor 568 conjugates, and all secondary antibodies were purchased from Molecular Probes. To visualize endocytic trafficking of dextran, Dextran Alexa Fluor 568 conjugate was presented to cells for 1 h at 37°C (1 mg/ml), followed by fixation immediately or after a 3-h chase with growth medium (1 + 3 h), which moves the dextran conjugate to late endosomal and lysosomal compartments (Kauppi *et al*., 2002). Transferrin Alexa Fluor 568 conjugate was added for 1 h (50 μg/ml) and followed by a 30-min chase with growth medium to label recycling endosomes (Sheff *et al*., 2002). Cells were examined using a confocal microscope (LSM 510; Carl Zeiss, Thornwood, NY) with a 63× C-Apochromat water objective (numerical aperture 1.2), and images were exported to Adobe Photoshop 7.0. Quantitative image analyses were performed using ImageJ 1.30v software (Wayne Rasband, National Institutes of Health, Bethesda, MD; http://rsb.info.nih.gov/ij/). Either the mean fluorescence per cell was determined or the ratio of total fluorescence associated with plasma membrane and intracellular compartment was calculated. For each image the background fluorescence was measured and subtracted.

Chemiluminescence Detection of Cell Surface Extope-CFTR

Cells were grown in 96-well black isoplates (PerkinElmer Life and Analytical Sciences) and incubated for 2 d at 27°C in the presence of 2 mM butyrate. Cells were washed twice in ice-cold PBS (Invitrogen) and precooled for 10 min on ice at 4°C. Anti-HA ascites (16B12) was added at 1:500 in ice-cold growth medium for 30 min on ice at 4°C. Cells were washed two times with ice cold medium and one time with ice cold PBS and reincubated with warm growth medium for the times indicated. Cells were then washed and fixed for 10 min in 4% paraformaldehyde. Cells were washed again five times by using an Auto Plate Washer Elx405 (Bio-Tek Instruments, Winooski, VT) and blocked in 1% BSA and 5% normal goat serum in PBS. Cells were incubated with anti-mouse IgG horseradish peroxidase conjugate (1:5000 for 1 h; Amersham Biosciences) and washed five times. Supersignal ELISA Pico chemiluminescence substrate (Pierce Chemical) was added and the luminescence was quantified using a Victor^2 1420 multilable counter. The effect of the proteasomal inhibitor lactacystin on internalization of Extope-CFTR was in principle tested similarly. Cells were preincubated for 1 h with lactacystin (25 μM), and cell surface pools of Extope-CFTR were labeled followed by reincubation in warm (37°C) growth medium with lactacystin for indicated times. Chemiluminescence was quantified with a TopCount NXT (PerkinElmer Life and Analytical Sciences).

RESULTS

External-Epitope–tagged CFTR Enables Direct Visualization of Endocytosis

Although the endocytosis of CFTR was demonstrated a decade ago (Bradbury *et al*., 1992; Lukacs *et al*., 1992) and has been extensively characterized since then (Swiatecka-Urban *et al*., 2002; Picciano *et al*., 2003, and references therein), the internalized protein has not been directly visualized, largely because of the paucity of reagents that specifically recognize the extracellular surface of the protein. To overcome this limitation, we modified the second extracytoplasmic loop of CFTR to contain an exposed epitope and designated this construct Extope-CFTR (Figure 1A). When stably expressed in BHK-21 cells this protein matured to a similar extent as unmodified wild type CFTR and is readily detected by an antibody recognizing the epitope (Figure 1B). The normal proportions of bands representing the polypeptide with core and complex oligosaccharide chains are observed. The increased size of both due to the insertion is also apparent. That this external-epitope–tagged CFTR retains cyclic AMP-stimulated chloride channel activity is shown in Figure 1C, where rates of $^{36}Cl^-$ efflux similar to those from cells ex-

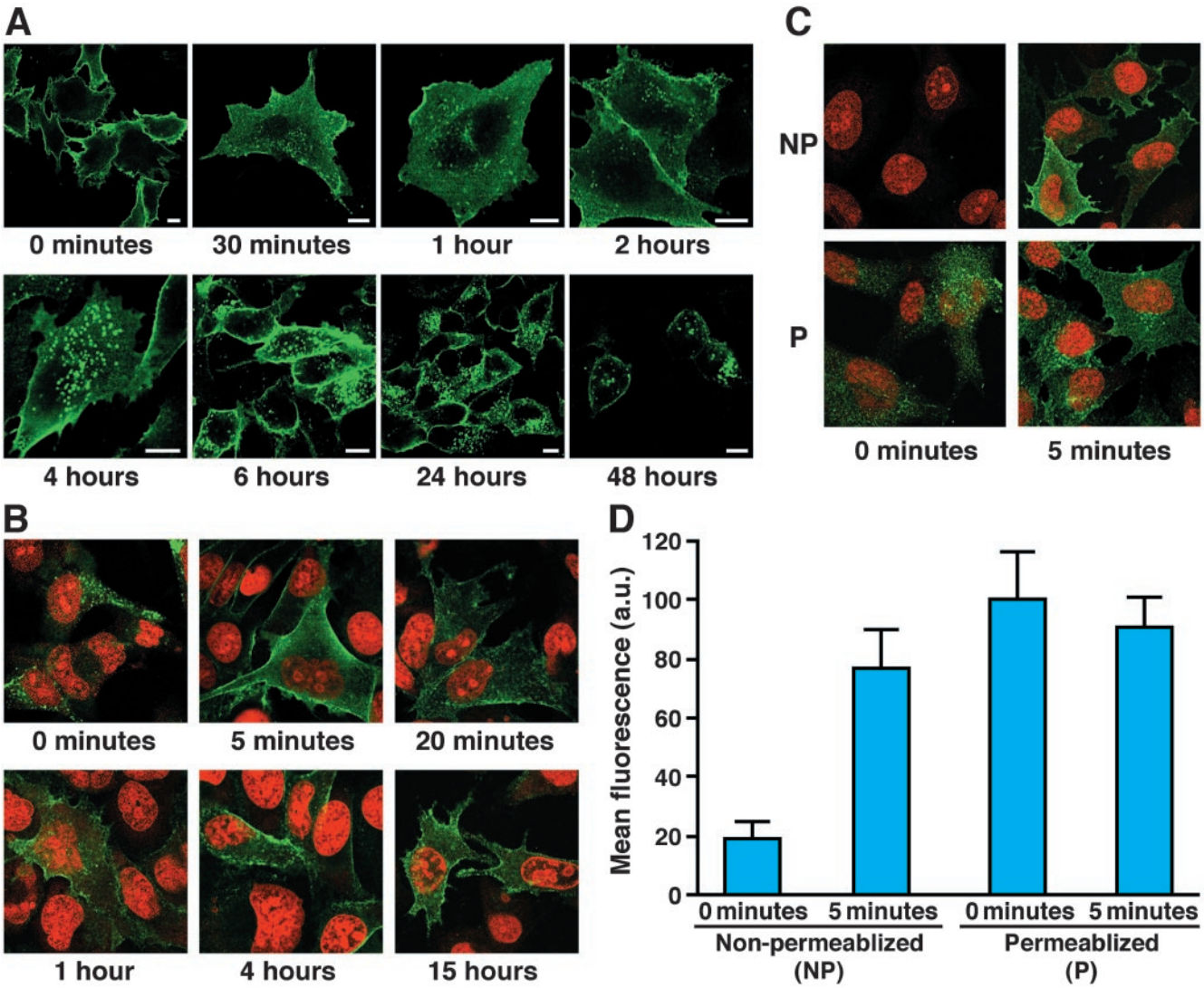

Figure 2. Extope-CFTR is internalized and recycled. (A) Cell surface pools of Extope-CFTR are internalized. BHK-21 cells stably expressing Extope-CFTR were precooled, and cell surface pools of Extope CFTR were labeled for 30 min on ice with mouse monoclonal anti-HA antibody 16B12. Cells were then washed with ice-cold PBS and reincubated for the indicated times. Bars, 10 μm. (B) Internalized pools of CFTR are rapidly recycled. Cells were labeled for 10 min with monoclonal mouse anti-HA antibody 12CA5 and then washed with PBS, pH 3.7, to remove antibody from the cell surface. Reincubatiuon in prewarmed media for different times results in reappearance of CFTR at the cell edges. Cells were fixed with 4% paraformaldehyde for 10 min and permeabilized with 0.1% saponin in PBS. Extope-CFTR labeled with 12CA5 mAb was detected with goat anti-mouse IgG conjugated to Alexa Fluor 488. Nuclei were stained with propidium iodide. (C) Recycled CFTR is redirected to the cell surface. Internalized Extope-CFTR is detectable at the cell surface of nonpermeabilized cells after 5-min reincubation in media. Extope-CFTR–expressing cells were labeled with 12CA5 and washed to remove external label as in Figure 2B. Cells were fixed immediately or after 5-min reincubation in warm media and either not permeabilized (NP) or permeabilized (P). Extope-CFTR labeled with 12CA5 mAb was immunostained by goat anti-mouse IgG conjugated to Alexa Fluor 488. (D) Quantification of CFTR recycling to the plasma membrane. The internalized pool of CFTR is almost completely redirected to the cell surface in 5 min. Experiments were performed as in Figure 2C, and mean green fluorescence per cell was determined as described in MATERIALS AND METHODS by using ImageJ 1.30v software. Each point represents the average of at least 10 cells and standard deviations are indicated.

pressing unmodified CFTR are observed. Figure 1D shows the precise labeling of the plasma membrane pool and endocytic compartments (left) in contrast to the broad distribution throughout the cell of the entire CFTR pool (right).

The redistribution of the surface pool was then followed over a period of 48 h by confocal immunofluorescence microscopy after labeling viable cells with an antibody to the inserted epitope (Figure 2A). Within 0.5 h or less, considerable intracellular staining became apparent, largely in association with small vesicles beneath the plasma membrane (Figure 2A; quantified in Supplemental Figure 3A). These remained at 1 and 2 h when some larger punctate structures also began to occur. By 4 h, concentration in these distinct larger punctate structures deeper in the cell interior was obvious and these remained at later times (6, 24, and 48 h). Considerable labeling at the plasma membrane was present even after the longest time periods. This could reflect a residual amount of the initial surface pool or material that has returned from internal pools or both. Very similar staining patterns were ob-

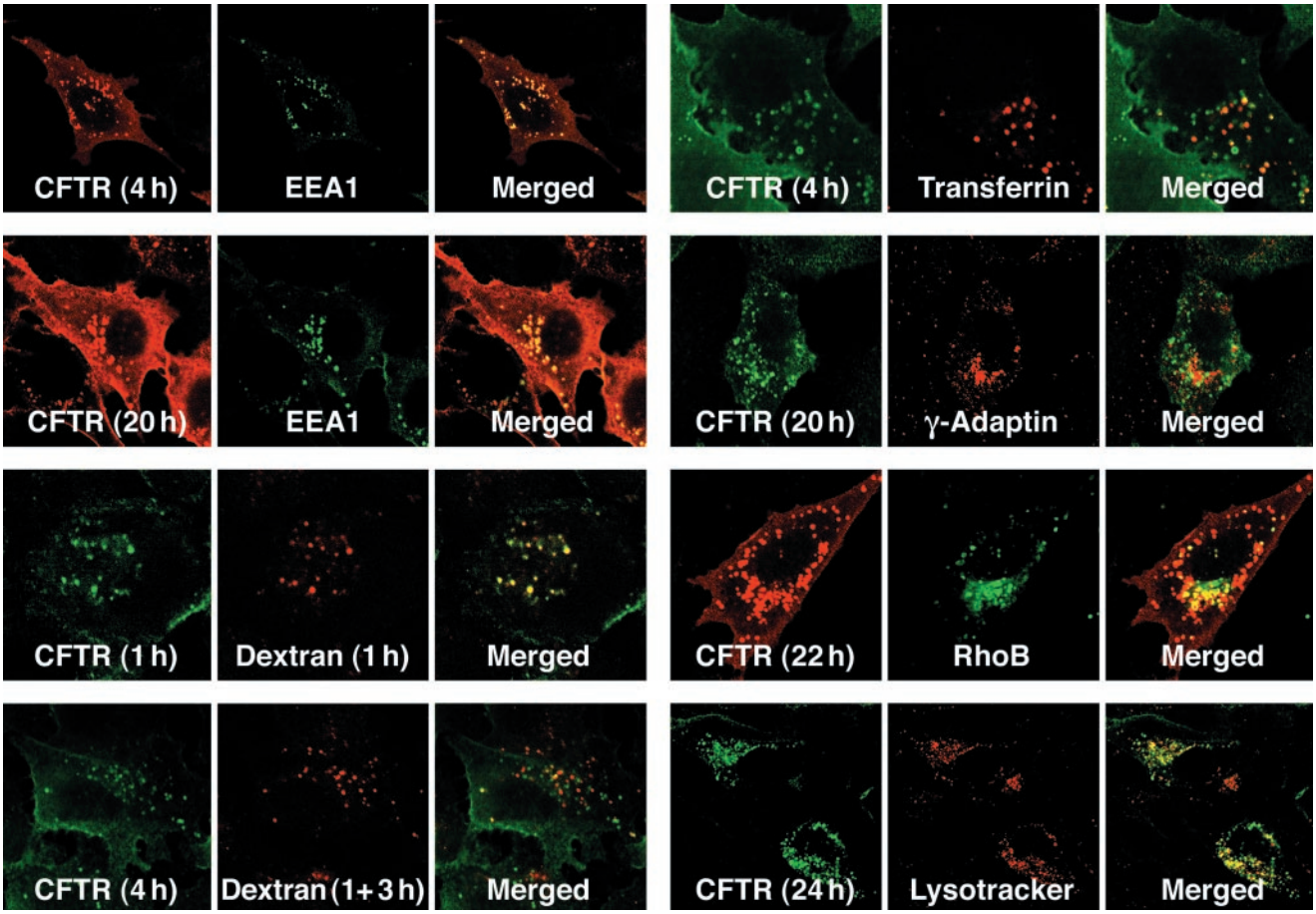

Figure 3. Localization of internalized CFTR relative to organelle markers. Extope-CFTR was labeled on the cell surface with anti-HA antibody (16B12). Cells were reincubated and fixed after the indicated times. Cells were permeabilized, blocked, and internalized Extope-CFTR was immunostained as described in Figure 2A by using goat anti-mouse IgG Alexa Fluor 488 conjugate or goat anti-mouse Fab Alexa Fluor 568 for detection. Subcellular marker proteins were labeled as described in MATERIALS AND METHODS. EEA1 was detected with an antibody directly conjugated to fluorescein isothiocyanate, and γ-Adaptin was visualized using a rabbit antibody. RhoB was transiently expressed as a fusion to EGFP. Alexa Fluor 568-dextran conjugates were added to the medium for 1 h, and cells were either analyzed immediately or reincubated for another 3 h in regular medium (1 + 3 h). Transferrin Alexa Fluor 568 was added to the media for 1 h followed by a 30-min chase with regular media. Lysosomes were detected with Lysotracker Red.

tained using Fab fragments rather than the complete 16B12 antibody, indicating that the endocytic trafficking events were not influenced by any cross-linking with bivalent Ig that might occur (Supplemental Figure 1).

Internalized CFTR Is Redirected to the Plasma Membrane

To test whether Extope-CFTR is recycled to the plasma membrane, antibody bound at the surface was removed by acid washing (Supplemental Figure 2). After Extope-CFTR was labeled with anti-HA mAb 12CA5 for 10 min in growth media followed by a wash with PBS, pH 3.7, only intracellular label was detected (Figure 2B, 0 minutes). Reincubation of the cells resulted in a movement of internalized Extope-CFTR to the cell edges, with the amount at the cell membrane already maximal after 5 min (Figure 2B; quantified in Supplemental Figure 3B). This population was accessible to staining with secondary antibody even in nonpermeabilized cells (Figure 2C), confirming that it is in the plasma membrane. Quantification of the detectable amount of Extope-CFTR in permeabilized and nonpermeabilized cells shows that the internalized pool of CFTR is almost completely redirected to the plasma membrane within 5 min (Figure 2D).

Localization of Internalized CFTR

To assess the multiple intracellular compartments in which plasma membrane-derived CFTR occurs, staining with different organellar markers was performed. The most complete colocalization was observed with EEA1 in early endosomes where much of the internalized CFTR is seen by 4 h and some remains at 20 h (Figure 3 and Supplemental Table 1). Comparison with the uptake of fluorescent dextran was used to confirm this because it is known to be primarily in early endosomes after 1 h and then move on to late endosomes after a 3-h chase (Kauppi *et al*., 2002). CFTR colocalizes with the dextran to early endosomes (at 1 h), whereas after the 3-h chase, it still remains mainly in the early endosomes so that the two then overlap minimally. At later time (4 h), a small amount of endocytosed CFTR colocalized with transferrin, suggesting involvement of recycling endosomes (Yamashiro *et al*., 1984; Sheff *et al*., 1999, 2002). Staining with the *trans*-Golgi network marker γ-Adaptin revealed that at late times (20 h), some of the endocytosed CFTR has accumulated very near the TGN. This seems reasonable because it is known that the TGN, and endosomes are in proximity

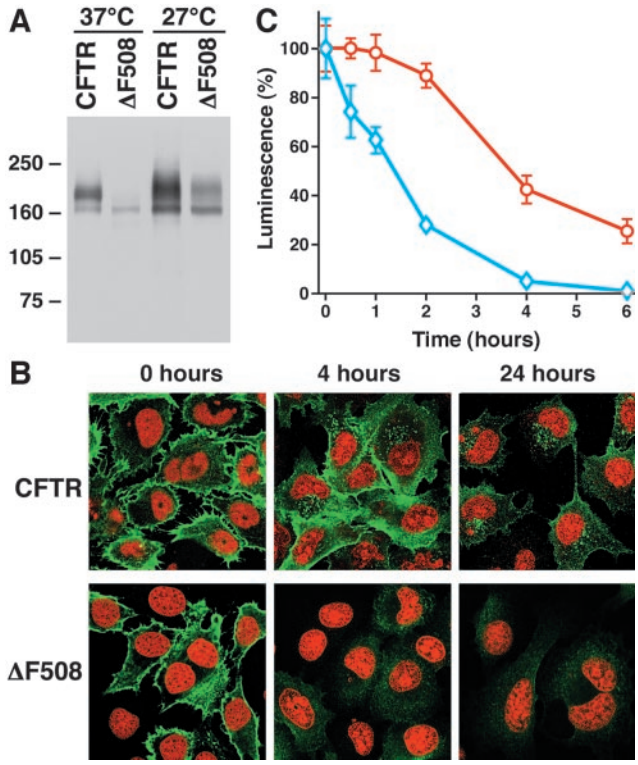

Figure 4. Turnover of ΔF508-CFTR at the cell surface differs from wild type CFTR. (A) Extope-ΔF508 CFTR matures at low temperature. Cells expressing Extope-CFTR and Extope-ΔF508 CFTR were grown at 37 or 27°C in the presence of 2 mM butyrate to increase expression, and cell lysates were analyzed by immunoblotting as described in Figure 1B by using anti-CFTR antibody 596. (B) Localization of Extope-CFTR and Extope-ΔF508 CFTR at different times after external labeling. BHK-21 cells stably expressing Extope-CFTR and Extope-ΔF508 CFTR were grown at 27°C in the presence of 2 mM butyrate. Extope-CFTR and the ΔF508 variant were labeled at the cell surface and visualized as described in MATERIALS AND METHODS at the times indicated. Nuclei were stained with propidium iodide. (C) Chemiluminescence detection of cell surface Extope-CFTR and Extope-ΔF508 CFTR. Extope-CFTR was labeled with anti-HA antibody 16B12 on cells, which had been grown at 27°C in the presence of butyrate. Cells were then reincubated at 37°C for the times indicated. Remaining Extope-CFTR (red circles) and Extope-ΔF508 (blue diamonds) on the cell surface were detected using sheep anti-mouse IgG horseradish peroxidase conjugate and chemiluminescence substrate as described in MATERIALS AND METHODS. Each point represents the average of eight wells and standard deviations are indicated.

and that material is exchanged between them by both anterograde and retrograde routes (Rohn *et al*., 2000). Also at ~1 d after endocytosis a small amount of CFTR colocalizes with Rho B in late endosomes and with Lysotracker Red in lysosomes. Therefore, at least some of the internalized protein apparently proceeds from early to late endosomes and to lysosomes for degradation.

Differential Turnover of Cell Surface Pools of Wild-Type and ΔF508 CFTR

Under normal conditions, ΔF508 CFTR does not reach the plasma membrane. However, in cells grown at reduced temperature or exposure to certain chemicals, conformational maturation and transport to the cell surface occurs (Gelman and Kopito, 2002). When BHK-21 cells stably expressing the external-epitope tagged ΔF508 CFTR were grown at 27°C, considerable maturation occurred (Figure 4A). The mature mutant protein reached the plasma membrane of many cells as evidenced by staining with external antibody (Figure 4B). When this signal was followed over time, however, it completely disappeared from the surface much more rapidly than the wild type. Furthermore, no significant stable residence in early endosomes, exhibited by the endocytosed wild type protein, was detected. By 24 h, very little endocytosed mutant protein was detectible at any location in these cells. In addition to these confocal immunofluorescence observations, we quantified the rates of disappearance of Extope-CFTR and Extope-ΔF508 CFTR from the cell surface by using a chemiluminescence-based epitope detection assay (Figure 4C). This reveals that although the steady-state population of cell surface wild type molecules decreases only by ~10% >2 h, ~75% of the mutant is removed during this period. By 4 h, virtually no mutant protein is detected in this assay, whereas there is still 40% of the initial amount of the wild type.

CFTR Endocytosis Is Blocked at Different Steps by Low Temperature and Protease Inhibitors

Because the ΔF508 mutant protein, in contrast to wild type CFTR, disappeared from the cell surface rapidly and was not detectable in significant amounts intracellularly, we attempted to determine whether an altered endocytic routing was responsible for this altered kinetics.

It has been shown for many cell types that temperatures between 16 and 22°C block degradation of endocytosed proteins by preventing their transport from endosomes to lysosomes (Dunn *et al*., 1980; Marsh *et al*., 1983; Parton *et al*., 1989). Under these conditions, endocytosed material localizes to EEA1-positive early endosomes (Sharma *et al*., 2003). When ΔF508 CFTR was labeled on cells shifted to 16°C, the protein accumulated in intracellular structures with similar appearance as the endosomal compartment where the wild-type protein was detected (Figure 5A).

Previous studies have shown that the turnover of immature and mature wild type CFTR is inhibited by proteosomal and lysosomal protease inhibitors, respectively (Lukacs *et al*., 1992; Ward *et al*., 1995). Extensive more recent investigations with a variety of different endocytosed membrane proteins have revealed a sensitivity to proteasome inhibitors at at least two steps in the endocytic pathway (Bonifacino and Traub, 2003) as well as to inhibitors of lysosomal proteases that are directly responsible for degradation of endocytosed proteins. Therefore, we tested the effects of both classes of inhibitors on the endocytosis of wild type and mutant CFTR pools during an intermediate time period (7 h) of endocytosis when wild type Extope-CFTR was widely distributed intracellularly, principally in early endosomes and still at the cell surface, whereas Extope-ΔF508 CFTR had already been reduced to very low levels (Figure 5B, controls). The most striking effects were exhibited by the ΔF508 protein on treatment with proteasomal inhibitors lactacystin and MG132 (Figure 5B), which resulted in retention of strong surface and subsurface signals similar to the initial staining at "0 time" (Figure 4B). Although not as dramatic, the effects of these compounds on the wild type protein were similar, resulting in very strong surface localization similar to that after initial labeling (Figure 2). These effects may reflect ubiquitin-dependent steps involved in the initial internalization and/or late endosome to lysosomal stages, which are implicated in the endocytic trafficking of other proteins (Katzmann *et al*., 2002; Hicke and Dunn, 2003), or as yet unidentified steps. To independently quantify CFTR

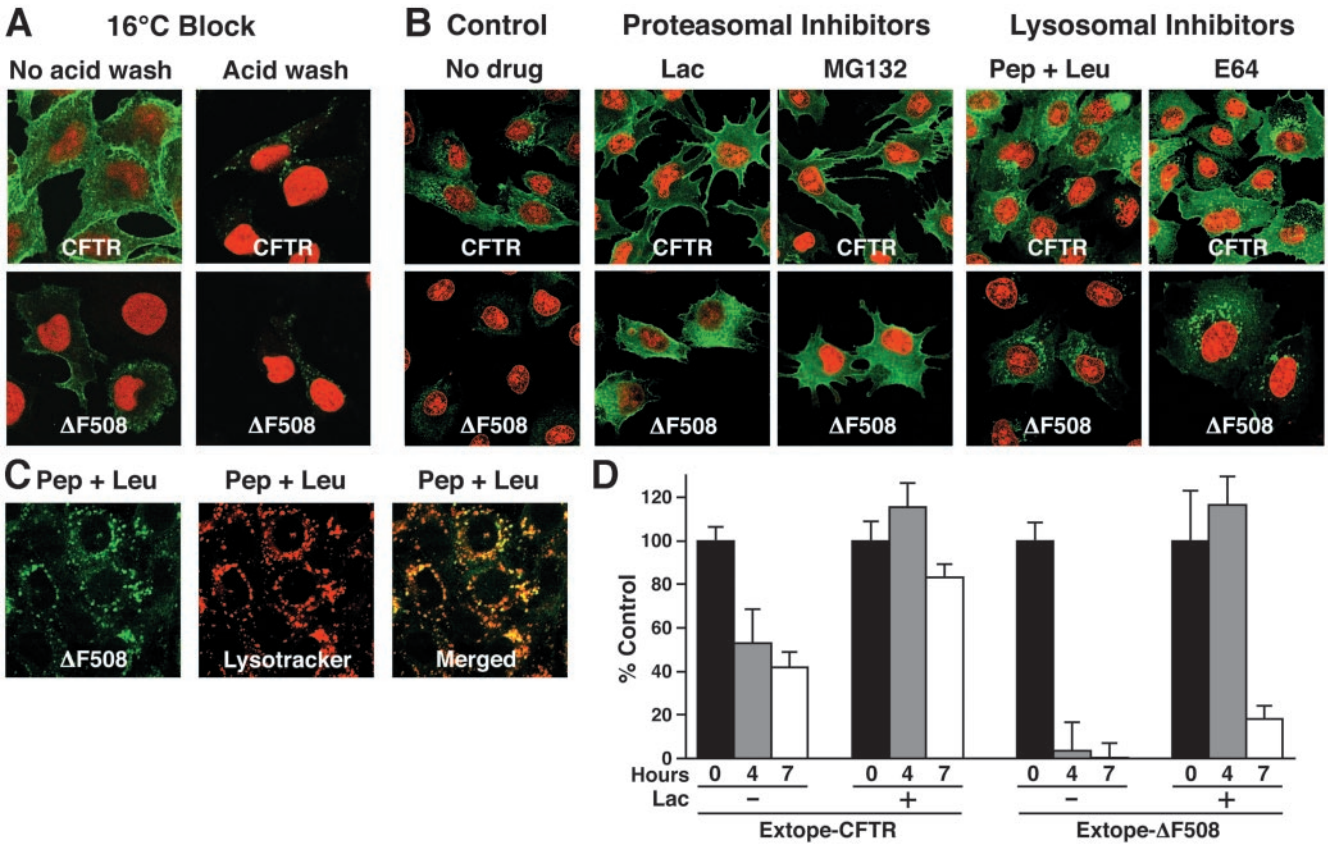

Figure 5. CFTR endocytosis is inhibited by low temperature and protease inhibitors. (A) Incubation of 16°C blocks endocytosis and allows intracellular detection of ΔF508-CFTR. Cells were grown at 27°C with 2 mM butyrate and incubated for 45 min at 16°C. Then, cell surface pools of Extope-CFTR and Extope-ΔF508 CFTR were labeled with 12CA5 mAb for 30 min at the same temperature. Subsequently cells were washed and reincubated in regular media for 1 h. Extope-CFTR was then detected in cells washed with regular PBS, pH 7.4 (no acidic wash), or after an acidic wash (acidic wash). Nuclei were stained with propidium iodide. (B) Lysosomal and proteasomal inhibitors inhibit endocytic turnover of ΔF508-CFTR. Cell surface Extope-CFTR or Extope-ΔF508 CFTR were labeled with 16B12 as described in Figure 2A. Cells were reincubated at 37°C for 7 h with either lysosomal inhibitors pepstatin-A and leupeptin (Pep + Leu, each 50 μg/ml) and E64 (3.5 μg/ml) or proteasomal inhibitors lactacystin (50 μM) and MG132 (50 μM) or without drug (control) and stained for immunofluorescence microscopy. Nuclei were stained with propidium iodide. (C) ΔF508 CFTR accumulates in lysosomes in the presence of the lysosomal inhibitors. Cells were treated with lysosomal inhibitors pepstatin-A and leupeptin as described in Figure 5B. Extope-ΔF508 CFTR was labeled with 16B12 at the cell surface and detected 7 h later by using goat anti-mouse IgG Alexa Fluor 488 conjugate. Lysosomes were labeled with Lysotracker Red (Molecular Probes). (D) Proteasomal inhibitor increases the amount of CFTR retained at the cellular surface. Extope-CFTR and ΔF508 CFTR were labeled on intact precooled cells on ice for 30 min with 16B12 mAb and cells were reincubated in the presence or absence of lactacystin (25 μM) for indicated times. Cell surface Extope-CFTR was detected in a chemiluminescence assay at indicated times by using sheep antimouse peroxidase conjugate and chemiluminescence (see MATERIALS AND METHODS). Each experiment was performed with 8 replicates and standard deviations are indicated.

trapped at the plasma membrane in the presence of a proteasomal inhibitor, cell surface pools were labeled and the disappearance from the cell surface was monitored with a chemiluminescence assay. The proteasomal inhibitor lactacystin indeed stabilized the cell surface pool of ΔF508 dramatically and also increased the amount of wild type CFTR (Figure 5D). The presence of proteasomal inhibitor resulted in detection of the same amount of ΔF508 after 4 h as at time 0, whereas in the absence of inhibitor it had disappeared almost completely from the cell surface.

The lysosomal protease inhibitors caused some increase in intracellular pools of wild type CFTR, but they also have a more drastic effect on ΔF508 CFTR, resulting in the appearance of significant amounts of intracellular endocytosed protein as strong intracellular punctated staining (Figure 5B), whereas without treatment only a faint submembranous sprinkling (ΔF508 control) was detectable. The structures, where ΔF508 CFTR is found in the presence of the lysosomal inhibitors, also were stained with Lysotracker Red, identifying them as lysosomes (Figure 5C). This accumulation in lysosomes on inhibition of lysosomal proteases indicates that these are ultimately responsible for degradation of the rapidly endocytosed mutant protein. The overall amount of the wild type protein remaining is also slightly increased by both pepstatin plus leuptin and E64, indicating that it also succumbs to lysosomal proteins albeit at a much slower rate than the mutant (Figure 5B). Overall, these experiments revealed no major change in the endocytic itinerary of ΔF508 CFTR despite its much more rapid turnover relative to the wild type protein.

Rab Proteins Reveal CFTR Endocytic Routing

Different Rab small GTPases are known to control vesicular fusion at various stages in the endocytic cycle (Pfeffer, 2001; Zerial and McBride, 2001; Choudhury *et al*., 2002) and there-

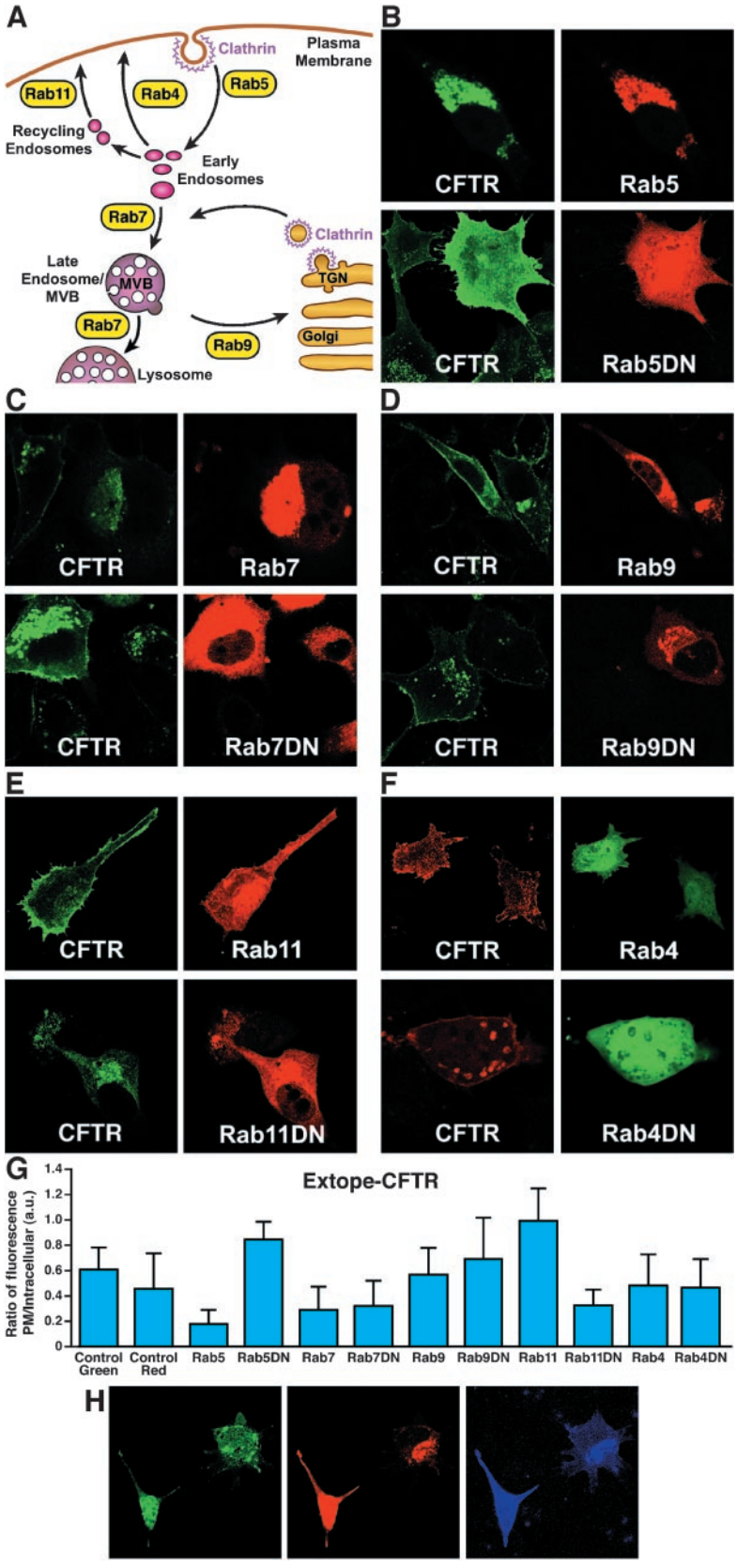

Figure 6. Influence of Rab proteins on the endocytic routing of CFTR. (A) Cartoon indicating endocytic routes regulated by Rab proteins. Rab5 directs transport from the plasma membrane to endocytic vesicles and fusion of early endosomes. Rab7 mediates early-to-late endosome and late endosome-to-lysosome transport, and Rab9 is involved in transport from endosomes to the *trans*-Golgi network. Rab11 and Rab4 mediate recycling back to the plasma membrane: Rab4 controls a rapid direct recycling route from early endosomes to the cell surface and Rab11 catalyzes a recycling route through recycling endosomes to the plasma membrane. (B–F) Influence of wild type and dominant negative (DN) Rab variants. Rab proteins were transiently overexpressed as fusions with DsRed (Rab5, 7, 9, 11, and DN mutants) or as fusions with EGFP (Rab4 and Rab4DN). Extope-CFTR was labeled at the cell surface 24 h after transfection and detected 24 h later by immunofluorescence. Rab proteins overexpressed were Rab5a and Rab5aN133I (B), Rab7 and Rab7T22N (C), Rab9 and Rab9S21N (D), Rab11 and Rab11S25N (E), and Rab4a and Rab4aN121I (F). (G) Quantification of experiments shown in Figure 6, B–F: Rab GTPases effect cellular distribution of CFTR. Image analysis using ImageJ 1.30v software was performed to determine the ratio of fluorescence associated with plasma membrane to intracellular pools on overexpression of different Rab GTPases. Extope-CFTR was either labeled with secondary antibody conjugated to Alexa Fluor 488 (control green and on overexpression of Rab5, Rab7, Rab9, Rab11, and DN mutants) or Alexa Fluor 568 (control red, Rab4, and Rab4DN). Each point represents the average of at least 10 cells, and standard deviations are indicated. (H) Endocytosed CFTR colocalizes with Rab11, but not Rab4. Rab11 (DsRed fusion) and Rab4 (EGFP fusion) were transiently coexpressed in Extope-CFTR–expressing cells and labeling of Extope-CFTR was performed as described in Figure 6, B–F. Extope-CFTR, detected after 24 h by using a goat anti-mouse Alexa Fluor 633 conjugate, is shown in blue. Rab11 colocalizes on low expression with endocytosed CFTR, but not Rab4 (right cell), whereas high expression of Rab11 results in a bright staining of labeled CFTR at the cell surface (left cell).

fore serve as useful tools to elucidate the routes taken by internalized molecules. A schematized depiction of their sites of action is shown in Figure 6A. To determine the influence of Rab proteins on Extope-CFTR endocytosis, we transiently overexpressed both wild type and dominant negative mutant Rab protein versions, labeled with external antibody 24 h after transfection and detected labeled CFTR 24 h later (Figure 6, B–F, quantified in Figure 6G). Rab5a controls the transport from the plasma membrane to endocytic vesicles and the homotypic fusion between early endosomes and its overexpression relocates cell surface CFTR to an intracellular location, where it colocalizes with Rab5a (Figure 6B). Rab5a resides mainly in early endosomes and its overexpression is known to increase the size of that compartment (Stenmark *et al*., 1994; Roberts *et al*., 1999). On overexpression of a dominant-negative Rab5a mutant (Rab5aDN), endocytosis of CFTR is drastically inhibited and CFTR labeled at the cell surface stays associated with the plasma membrane or immediately beneath it, indicating that CFTR endocytosis is Rab5a dependent.

Rab7 mediates early-to-late endosome and late endosome-to-lysosome transport. When overexpressed, dominant negative Rab7 (Rab7DN) greatly increased the entire intracellular CFTR pool (Figure 6C). In contrast, the wild type protein caused a decrease of the plasma membrane and endosomal pools of CFTR, consistent with a promotion of degradation. This confirms that after uptake to early endosomes a major routing of CFTR is on to late endosomes and then to lysosomes where it is proteolysed.

The GTPase Rab9 is involved in transport from endosomes to the TGN and interestingly Rab9 overexpression increased both cell surface and intracellular staining significantly. Within cells in which Rab9 was overexpressed CFTR occurred not only in early endosomes but also and to a greater extent in a different compartment, which overlaps with the TGN marker γ-Adaptin (our unpublished data). The Rab9 dominant negative mutant had a qualitatively similar effect as wild type Rab7 with reduction of the CFTR pool (Figure 6D), suggesting that relocation of CFTR to the TGN stabilizes subcellular pools.

Rab4 and Rab11 seem to overlap partially in their localization along the endocytic pathway but catalyze different recycling routes to the plasma membrane (Sonnichsen *et al*., 2000). Rab4 seems to control a rapid direct recycling route from early endosomes to the cell surface (van der Sluijs *et al*., 1992; Sheff *et al*., 1999), and Rab11 mediates recycling from recycling endosomes to the plasma membrane (Ullrich *et al*., 1996). Overexpression of Rab11 moved most of the endocytosed CFTR molecules back to the plasma membrane (Figure 6E). A dominant negative Rab11 mutant had the opposite effect: cell surface labeling disappeared almost completely, whereas intracellular pools were increased. Rab4a overexpression had only a minor effect on the CFTR cell surface pool (Figure 6F). On overexpression of Rab4aDN, the size of the endosomal compartment to which CFTR localizes increased significantly. This change in appearance and increase in size of early endosomes have been observed previously on overexpression of Rab4DN and are most likely caused by the accumulation of proteins in early endosomes as a consequence of their inability to be recycled (van der Sluijs *et al*., 1992; Mohrmann *et al*., 2002). More significantly, even on block of the Rab4-dependent recycling route, there is still as much CFTR associated with the plasma membrane as in nontransfected cells.

From the above-mentioned observations, it seemed that the Rab11- rather than the Rab4-controlled route is dominant in the recycling of CFTR to the cell surface. To test this further, the same type of experiment was performed with coexpression of the wild type versions of both these GTPases. Because these were expressed transiently, their amounts varied among cells. For example, in Figure 6H, one cell is seen to express Rab11 at a low level (right cell) with CFTR colocalizing presumably in recycling endosomes, very distinct from the Rab4 distribution. In the other cell (left), in which Rab11 is strongly expressed, CFTR is predominantly at the cell surface as was the case in the absence of Rab4.

Modulation of Rab5- and Rab11-controlled Steps Stabilize ΔF508 CFTR at the Cell Surface

Overall, these experiments reveal that CFTR enters several different endocytic routes: Rab5a regulated internalization, Rab11-dependent recycling to the plasma membrane, a degradative pathway to lysosomes, and a Rab-dependent retrieval route from late endosomes to the TGN. Accordingly, the overexpression of RabGTPases or their dominant negative mutants involved in these routes result in a subcellular redistribution of Extope-CFTR in the endocytic pathway (Figure 6).

Rab5DN and Rab11 overexpression seemed to cause the most drastic increase in the CFTR pool associated with the cell surface. Two additional experiments were performed to determine whether CFTR under these circumstances indeed resides at the plasma membrane. First, Extope-CFTR in intact Rab5-expressing cells was labeled with antibody and 4 h later detected in permeabilized and also nonpermeabilized cells where in both cases it was localized to the plasma membrane (Figure 7A). Acidic stripping of the antibody resulted in the inability to detect Extope-CFTR in permeabilized Rab5DN-expressing cells. This indicates that CFTR endocytosis is entirely blocked on overexpression of Rab5DN and that the CFTR remains at the plasma membrane.

In a second type of experiment, we sought to gain further direct evidence that Rab11 causes a redistribution of internalized CFTR to the cell surface. CFTR in Rab11-expressing cells was labeled for 10 min in growth medium, and the label was subsequently removed from the cell surface pool by an acidic wash, so that only intracellular CFTR was labeled (Figure 7B, 0 h). After reincubation, labeled CFTR was detected 4 h later in permeabilized and also nonpermeabilized cells, confirming that intracellular CFTR had been redistributed to the cell surface in Rab11-expressing cells.

Because Rab11 and Rab5aDN caused the greatest increase in wild type CFTR at the cell surface, we tested their influence on ΔF508 CFTR. Augmentation of internalization by overexpression of wild type Rab5a or inhibition of recycling by overexpression of Rab11DN did not change the rapid elimination of the ΔF508 protein (Figure 8, A and B) that already occurs without introduction of these Rabs (Figure 4B). Strikingly, however, not only block of endocytosis by Rab5aDN overexpression (Figure 8A) but also increasing the recycling pathway by overexpression of Rab11 (Figure 8B) resulted in substantial accumulation of the mutant channel protein at the cell surface. These findings demonstrate that although the mutant CFTR is not normally effectively recycled to the plasma membrane, this can occur when the recycling pathway is enhanced. As with wild type CFTR overexpression of Rab4 caused no significant stabilization of ΔF508 CFTR (Figure 8C). Rab7DN overexpression caused an accumulation of ΔF508 CFTR in intracellular structures, which may be either endosomes or lysosomes, but not at the cell surface (Figure 8D).

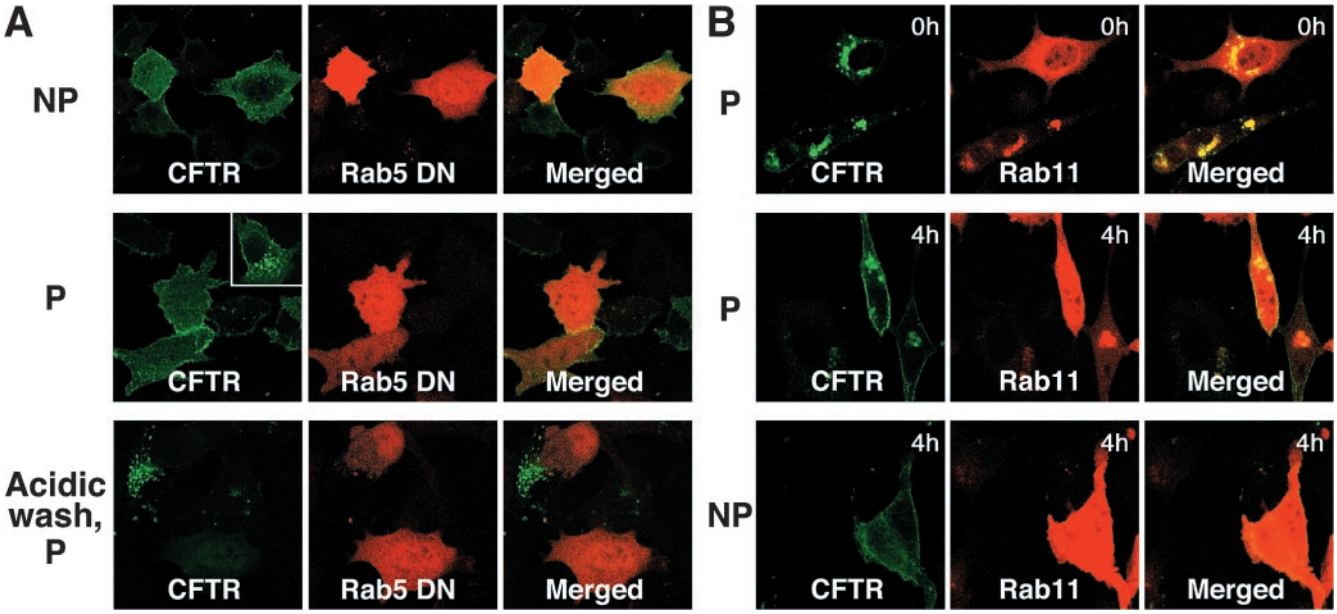

Figure 7. Extope-CFTR remains at or is recycled to the cell surface on overexpression of Rab5 DN or Rab11. (A) Extope-CFTR is trapped at the cell surface on overexpression of Rab5DN. Cells were transfected with Rab5aDN and 24 h later labeled for 10 min with 12CA5 mAb. Extope-CFTR was detected 4 h after labeling with mAb in nonpermeabilized (NP) or permeabilized (P) cells. A typical nontransfected cell is shown as an inset in the panel with permeabilized cells. No intracellular Extope-CFTR could be detected in permeabilized cells when cell surface mAb label was removed by acidic wash before fixation and permeabilization. (B) Extope-CFTR is robustly recycled to the plasma membrane on overexpression of Rab11. Cells were transfected with Rab11 and 24 h later intact cells were labeled for 10 min with mAb 12CA5. The mAb bound to the cells surface pool of Extope-CFTR was then removed by an acidic wash. Cells were either fixed and immediately immunostained (0 h) or reincubated in media for 4 h (4 h). Extope-CFTR was then detected in permeabilized or nonpermeabilized cells.

DISCUSSION

Because CFTR mislocalization due to aberrant intracellular transport is responsible for most cystic fibrosis, elucidation of the mechanisms regulating this transport is potentially of practical as well as theoretical importance. Although the most common disease-causing mutant, ΔF508, is retained in the proximal secretory pathway, there seems to be a fairly direct transport of the wild type from the ER to the TGN in the distal pathway in at least some cell types (Yoo *et al.*, 2002). This newly synthesized protein then travels in secretory vesicles to the plasma membrane. Early studies showed that whereas the overall pool in the distal pathway was very stable ($t_{1/2}$ of ~16 h; Lukacs *et al.*, 1993), the portion that could be chemically labeled from the external surface of the plasma membrane disappeared within minutes (Prince *et al.*, 1994; Lukacs *et al.*, 1997). Conditions that blocked endocytosis inhibited this rapid disappearance (Lukacs *et al.*, 1997). Using similar methods ΔF508 CFTR that had reached the cell surface in cells grown at reduced temperature was shown to be less stable than the wild type. This already indicated that the mutant polypeptide is recognized as distinct from the wild type in the distal as well as the proximal secretory pathway just as Benharouga *et al.* (2001) have shown to be the case for C-terminal truncation mutants of CFTR. As mentioned repeatedly by other investigators studying the mechanisms and routings of CFTR in the endocytic pathway, the lack of antibodies to extracellular domains of CFTR has precluded direct monitoring of its movement from the cell surface to other endocytic compartments. We have now overcome this limitation by engineering wild type and ΔF508 constructs with an externally accessible epitope in an expanded extracytoplasmic loop without compromising maturation, glycosylation, trafficking, and function. This has enabled direct focus on the cell surface pool distinct from the total cellular CFTR pool.

This approach has provided clear-cut confirmation of several features of CFTR endocytosis obtained by more indirect assays and revealed new information about different routings in the endocytic pathway and apparent relationships between them. By following the surface pool in the confocal microscope over time and its relationship to markers of different membranous compartments, portions of plasma membrane-derived CFTR were observed in a uniform population of small vesicles beneath the surface, early and recycling endosomes, late endosomes in proximity to the TGN as well as a small amount together with a TGN marker itself, especially when movement from endosomes to the TGN was promoted by Rab9. Surface-derived ΔF508 could only be detected distributed among multiple intracellular pools after blocking of endocytosis with low temperature or either inhibitors of lysosomal proteases or the proteasome. At 16°C, ΔF508 CFTR accumulates intracellularly in early endosomes like wild type CFTR. The stabilization of intracellular ΔF508 CFTR by lysosomal proteases inhibitors is not surprising because mature wild type CFTR is known to be degraded by lysosomal proteases (Lukacs *et al.*, 1992). ΔF508 CFTR, which matures under artificial conditions (low temperature, in this case), apparently meets the same fate but at a much more rapid rate. The result can be altered, however, by either blocking or augmenting specific steps in the endocytic pathway by using different Rab proteins (see below).

The basis of the strong blockade by proteasome inhibitors of internalization and stabilization at the surface of both wild type and ΔF508 CFTR is less obvious, even though this is known to occur with an ever-increasing list of endocytosed membrane proteins (Rocca *et al.*, 2001; van Kerkhof *et*

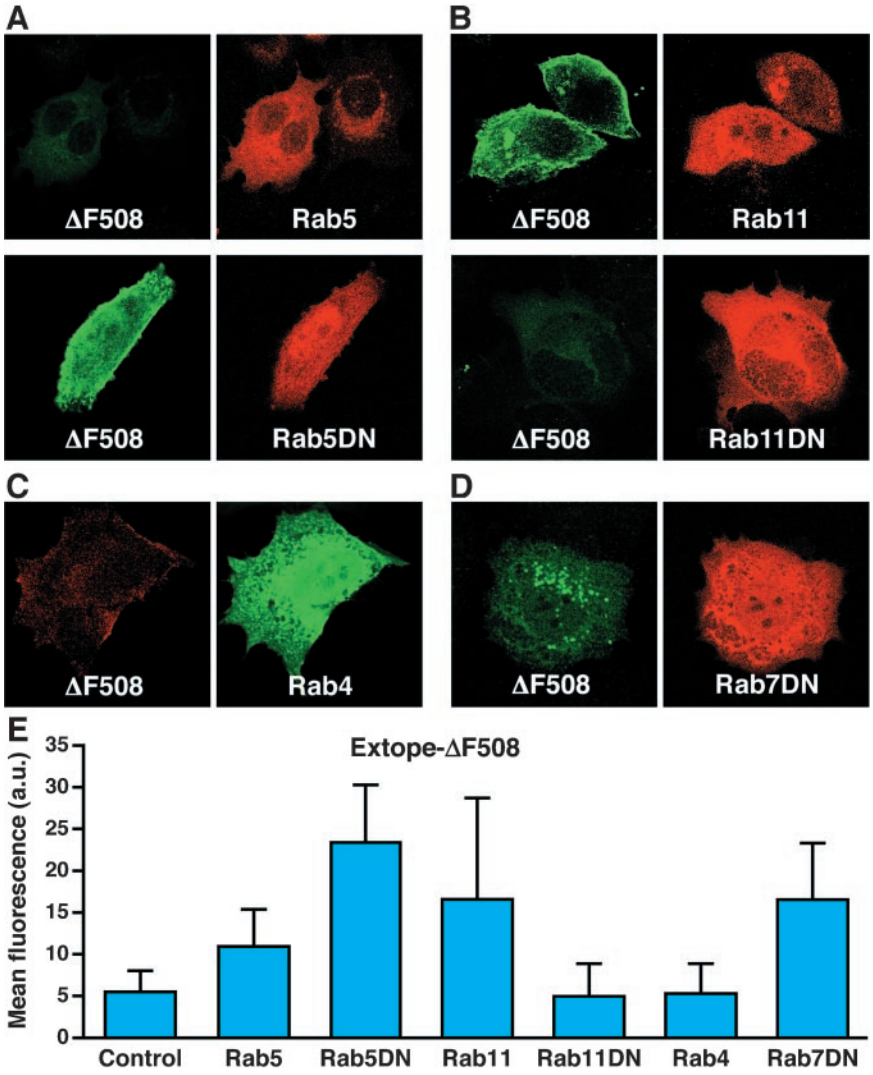

Figure 8. Rescue of the cell surface pool of ΔF508 CFTR by Rab11 and Rab5DN. Cells were grown at 27°C in the presence of butyrate and different Rab GTPases were transiently overexpressed as EGFP (Rab4) or DsRed (Rab5, Rab5DN, Rab11, Rab11DN, and Rab7DN) fusions. Extope-ΔF508 CFTR was labeled with 16B12 mAb as described in Figure 6 and detected 24 h later with goat anti-mouse IgG Alexa Fluor 488 conjugate or goat anti-mouse IgG Alexa Fluor 568 conjugate. (A) Rab5DN stabilized Extope-ΔF508 CFTR at the plasma membrane. (B) Rab11 increased cell surface Extope-ΔF508 CFTR. (C) Rab4 did not significantly change the turnover of Extope-ΔF508 CFTR. (D) Rab7DN overexpression stabilized intracellular pools of Extope-ΔF508CFTR. (E) Images were analyzed with ImageJ 1.30v software to determine the mean fluorescence per cell on overexpression of different Rab GTPases. Each point represents the average of at least 10 cells, and standard deviations are indicated.

al., 2001; Yu and Malek, 2001; Longva *et al*., 2002; Melman *et al*., 2002). At least some of these are monoubiquitinated at multiple sites enabling recognition by a number of proteins with UIM domains, including a clathrin-containing endosomal multiprotein complex (Haglund *et al*., 2003). There is not known to be any direct role of the proteasome in these events and the effect of proteasome inhibitors may reflect the depletion of ubiquitin pools due to the extensive accumulation of many ubiquitinated proteins in cells treated with proteasome inhibitors (Bonifacino and Traub, 2003). Although their principal effect was to cause CFTR accumulation at the surface, proteasome inhibitors are known to impede another ubiquitin-dependent step in the endocytic itinerary of other internalized proteins destined for lysosomal degradation: the engulfment of late endosomal vesicles by multivesicular bodies (Katzmann *et al*., 2002). The present data do not yet reveal whether any of the effect of these inhibitors on CFTR endocytic trafficking is at this step. However, with the ability to directly view endocytosed CFTR in different compartments, it was possible to further dissect some of the steps between them using the Rab GTPases that control them. The effect of Rab7 confirmed the importance of transit from late endosomes to lysosomes in determining the fate of the endocytosed CFTR pool: wild type Rab7 resulted in disappearance of nearly all CFTR originating at the surface, whereas Rab7DN stabilized the protein at lysosomes and further upstream. Whereas ΔF508 CFTR accumulates on treatment with lysosomal inhibitors or on overexpression of Rab7DN in intracellular compartments, the pool at the cell surface does not seem to increase significantly. This suggests that the mutant protein at that step of the endocytic pathway is not able to recycle back to the cell surface. Whether this is the case, because the ΔF508 CFTR proteins are marked for degradation by a specific signal like ubiquitination, or simply because at that step they have already passed sorting compartments from where they can be redirected for recycling, remains to be determined.

CFTR is endocytosed in clathrin-coated vesicles and not surprisingly block of that step by overexpression of Rab5aDN causes accumulation of CFTR and ΔF508 CFTR at the cell surface. Rab5 is found mainly in early endosomes, where it colocalizes with its effector EEA1 (Simonsen *et al*., 1998; Sonnichsen *et al*., 2000), a marker protein of early endosomes, which also showed the best colocalization with early internalized CFTR in our study.

A novel finding that could not necessarily have been predicted was the overall increase of CFTR caused by the overexpression of Rab9, which promotes movement from

endosomes to the TGN. Although this interpretation remains to be rigorously confirmed, this would imply that the incremental amount moved to the TGN was delivered to the plasma membrane perhaps by the same vesicular route used by newly synthesized CFTR or directly transported back to early endosomes. The fact that less CFTR was detected at the plasma membrane and in endosomes after expression of dominant-negative (DN) Rab9 may indicate that blockage of transit to the TGN interferes with the perpetuation of subcellular pools of CFTR and leads to increased degradation. Interestingly, even without the overexpression of Rab9, a small amount of the intracelluar CFTR pool was found to colocalize with γ-Adaptin at the TGN (Figure 3 and Supplemental Table 1).

Perhaps most striking among the effects of the different Rab proteins was that of Rab11, essential in the recycling of cargo from recycling endosomes to the plasma membrane. Picciano *et al.* (2003) have already provided evidence, using a DN form of the Rme-1 protein, which regulates recycling, that internalized wild type CFTR normally enters recycling endosomes and recycles back to the surface similarly as do transferrin receptors. Overexpression of wild type Rab11 resulted in an accumulation of surface CFTR, whereas the DN form had the opposite effect, leaving no CFTR detectible at the surface. In contrast Rab4, which regulates rapid direct recycling back from early endosomes to the plasma membrane, did not have this effect. For some proteins, it has been shown that Rab4-dependent recycling requires stimulation, like the presence of the growth factor platelet-derived growth factor in the case of recycling of $\alpha_v\beta_3$ integrin (Roberts *et al*., 2001) or insulin stimulation for recycling of Glut4 (Vollenweider *et al*., 1997) and therefore we cannot rule out the possibility that there might be conditions where CFTR could be recycled by Rab4 more efficiently. However, under the conditions of our experiments, we could not observe a significant role of Rab4 in CFTR recycling.

In addition to confirming the importance of wild type CFTR recycling by Rab11, we found that ΔF508 CFTR can also be recycled when the Rab11-dependent recycling machinery is up-regulated. This is significant because the rapid movements of the mutant protein from the cell surface to endosomes and lysosomes observed might have reflected its inability to enter the recycling arm of the pathway. However, our present observations indicate that the mutant like the wild type protein can be redirected to the surface when the traffic in different directions from endosomes is shifted. Indeed the redistributions that the Rab proteins bring about as well as the rescue of the surface CFTR pool by proteasome inhibitors provide hope that efforts to develop more specific means of stabilizing the surface pool may be successful.

ACKNOWLEDGMENTS

We thank Sharon Fleck and Marv Ruona for preparation of manuscript and figures, respectively. This work was supported by the National Institute of Diabetes and Digestive and Kidney Diseases of the National Institutes of Health. A.C. is supported by a fellowship from National Niemann Pick Disease Foundation.

REFERENCES

Benharouga, M., Haardt, M., Kartner, N., and Lukacs, G.L. (2001). COOH-terminal truncations promote proteasome-dependent degradation of mature cystic fibrosis transmembrane conductance regulator from post-Golgi compartments. J. Cell Biol. *153*, 957–970.

Bonifacino, J.S., and Traub, L.M. (2003). Signals for sorting of transmembrane proteins to endosomes and lysosomes. Annu. Rev. Biochem. *72*, 395–447.

Bradbury, N.A., Clark, J.A., Watkins, S.C., Widnell, C.C., Smith, H.S.T., and Bridges, R.J. (1999). Characterization of the internalization pathways for the cystic fibrosis transmembrane conductance regulator. Am. J. Physiol. *276*, L659–L668.

Bradbury, N.A., Jilling, T., Berta, G., Sorscher, E.J., Bridges, R.J., and Kirk, K.L. (1992). Regulation of plasma membrane recycling by CFTR. Science *256*, 530–532.

Brown, C.R., Hong-Brown, L.Q., and Welch, W.J. (1997). Strategies for correcting the delta F508 CFTR protein-folding defect. J. Bioenerg. Biomembr. *29*, 491–502.

Chang, X.-B., Cui, L., Hou, Y., Jensen, T.J., Aleksandrov, A.A., Mengos, A., and Riordan, J.R. (1999). Removal of multiple arginine-framed trafficking signals overcomes misprocessing of delta F508 CFTR present in most patients with cystic fibrosis. Mol. Cell *4*, 137–142.

Chang, X.-B., Hou, Y.-X., Jensen, T., and Riordan, J.R. (1994). Mapping of the cystic fibrosis transmembrane conductance regulator membrane topology by glycosylation site insertion. J. Biol. Chem. *269*, 18572–18575.

Chang, X.-B., Tabcharani, J.A., Hou, Y.-X., Jensen, T.J., Kartner, N., Alon, N., Hanrahan, J.W., and Riordan, J.R. (1993). Protein kinase A (PKA) still activates CFTR chloride channel after mutagenesis of all ten PKA consensus phosphorylation sites. J. Biol. Chem. *268*, 11304–11311.

Choudhury, A., Dominguez, M., Puri, V., Sharma, D.K., Narita, K., Wheatley, C.L., Marks, D.L., and Pagano, R.E. (2002). Rab proteins mediate Golgi transport of caveola-internalized glycosphingolipids and correct lipid trafficking in Niemann-Pick C cells. J. Clin. Investig. *109*, 1541–1550.

Denning, G.M., Anderson, M.P., Amara, J.F., Marshall, J., Smith, A.E., and Welsh, M.J. (1992). Processing of mutant cystic fibrosis transmembrane conductance regulator is temperature-sensitive. Nature *358*, 761–764.

Dunn, W.A., Hubbard, A.L., and Aronson, N.N., Jr. (1980). Low temperature selectively inhibits fusion between pinocytic vesicles and lysosomes during heterophagy of 125I-asialofetuin by the perfused rat liver. J. Biol. Chem. *255*, 5971–5978.

Gelman, M.S., and Kopito, R.R. (2002). Rescuing protein conformation: prospects for pharmacological therapy in cystic fibrosis. J. Clin. Investig. *110*, 1591–1597.

Haglund, K., Sigismund, S., Polo, S., Szymkiewicz, I., Paolo Di Fiore, P., and Dikic, I. (2003). Multiple monoubiquitination of RTKs is sufficient for their endocytosis and degradation. Nat. Cell Biol. *5*, 461–466.

Hämmerle, M.M., Aleksandrov, A.A., and Riordan, J.R. (2001). Disease-associated mutations in the extracytoplasmic loops of cystic fibrosis transmembrane conductance regulator do not impede biosynthetic processing but impair chloride channel stability. J. Biol. Chem. *276*, 14848–14854.

Hanrahan, J.H., Gentzsch, M., and Riordan, J.R. (2003). The cystic fibrosis transmembrane conductance regulator (ABCC7). In: ABC Proteins: From Bacteria to Man, ed. B. Holland, C.F. Higgins, K. Kuchler, and S.P.C. Cole, New York: Elsevier Science, 589–618.

Heda, G.D., Tanwani, M., and Marino, C.R. (2001). The Delta F508 mutation shortens the biochemical half-life of plasma membrane CFTR in polarized epithelial cells. Am. J. Physiol. *280*, C166–C174.

Hicke, L., and Dunn, R. (2003). Regulation of membrane protein transport to ubiquitin and ubiquitin-binding proteins. Annu. Rev. Cell. Dev. Biol. *19*, 141–172.

Howard, M., DuVall, M.D., Devor, D.C., Dong, J.Y., Henze, K., and Frizzell, R.A. (1995). Epitope tagging permits cell surface detection of functional CFTR. Am. J. Physiol. *269*, C1565–C1576.

Howard, M., Jiang, X., Stolz, D.B., Hill, W.G., Johnson, J.A., Watkins, S.C., Frizzell, R.A., Bruton, C.M., Robbins, P.D., and Weisz, O.A. (2000). Forskolin-induced apical membrane insertion of virally expressed, epitope-tagged CFTR in polarized MDCK cells. Am. J. Physiol. *279*, C375–C382.

Hu, W., Howard, M., and Lukacs, G.L. (2001). Multiple endocytic signals in the C-terminal tail of the cystic fibrosis transmembrane conductance regulator. Biochem. J. *354*, 561–572.

Katzmann, D.J., Odorizzi, G., and Emr, S.D. (2002). Receptor downregulation and multivesicular-body sorting. Nat. Rev. Mol. Cell. Biol. *3*, 893–905.

Kauppi, M., Simonsen, A., Bremnes, B., Vieira, A., Callaghan, J., Stenmark, H., and Olkkonen, V.M. (2002). The small GTPase Rab22 interacts with EEA1 and controls endosomal membrane trafficking. J. Cell Sci. *115*, 899–911.

Kopito, R.R. (1999). Biosynthesis and degradation of CFTR. Physiol. Rev. *79*, S167–S173.

Longva, K.E., Blystad, F.D., Stang, E., Larsen, A.M., Johannessen, L.E., and Madshus, I.H. (2002). Ubiquitination and proteasomal activity is required for transport of the EGF receptor to inner membranes of multivesicular bodies. J. Cell Biol. *156*, 843–854.

Lukacs, G.L., Chang, X.-B., Bear, C., Kartner, N., Mohamed, A., Riordan, J.R., and Grinstein, S. (1993). The ÐF508 mutation decreases the stability of cystic fibrosis transmembrane conductance regulator in the plasma membrane. Determination of functional half-lives on transfected cells. J. Biol. Chem. *268*, 21592–21598.

Lukacs, G.L., Chang, X.-B., Kartner, N., Rotstein, O.D., Riordan, J.R., and Grinstein, S. (1992). The cystic fibrosis transmembrane regulator is present and functional in endosomes. Role as a determinant of endosomal pH. J. Biol. Chem. *267*, 14568–14572.

Lukacs, G.L., Segal, G., Kartner, N., Grinstein, S., and Zhang, F. (1997). Constitutive internalization of cystic fibrosis transmembrane conductance regulator occurs via clathrin-dependent endocytosis and is regulated by protein phosphorylation. Biochem. J. *328*, 353–361.

Marsh, M., Bolzau, E., and Helenius, A. (1983). Penetration of Semliki Forest virus from acidic prelysosomal vacuoles. Cell *32*, 931–940.

Melman, L., Geuze, H.J., Li, Y., McCormick, L.M., Van Kerkhof, P., Strous, G.J., Schwartz, A.L., and Bu, G. (2002). Proteasome regulates the delivery of LDL receptor-related protein into the degradation pathway. Mol. Biol. Cell *13*, 3325–3335.

Mohrmann, K., Leijendekker, R., Gerez, L., and van Der Sluijs, P. (2002). rab4 regulates transport to the apical plasma membrane in Madin-Darby canine kidney cells. J. Biol. Chem. *277*, 10474–10481.

Parton, R.G., Prydz, K., Bomsel, M., Simons, K., and Griffiths, G. (1989). Meeting of the apical and basolateral endocytic pathways of the Madin-Darby canine kidney cell in late endosomes. J. Cell Biol. *109*, 3259–3272.

Pfeffer, S.R. (2001). Rab GTPases: specifying and deciphering organelle identity and function. Trends Cell Biol. *11*, 487–491.

Picciano, J.A., Ameen, N., Grant, B., and Bradbury, N.A. (2003). Rme-1 regulates the recycling of the cystic fibrosis transmembrane conductance regulator. Am. J. Physiol. *285*, C1009–C1018.

Prince, L.S., Workman, R.B., Jr., and Marchase, R.B. (1994). Rapid endocytosis of the cystic fibrosis transmembrane conductance regulator chloride channel. Proc. Natl. Acad. Sci. USA *91*, 5192–5196.

Riordan, J.R. (1999). Cystic fibrosis as a disease of misprocessing of the cystic fibrosis transmembrane conductance regulator glycoprotein. Am. J. Hum. Genet. *64*, 1499–1504.

Roberts, M., Barry, S., Woods, A., van der Sluijs, P., and Norman, J. (2001). PDGF-regulated rab4-dependent recycling of alphavbeta3 integrin from early endosomes is necessary for cell adhesion and spreading. Curr. Biol. *11*, 1392–1402.

Roberts, R.L., Barbieri, M.A., Pryse, K.M., Chua, M., Morisaki, J.H., and Stahl, P.D. (1999). Endosome fusion in living cells overexpressing GFP-rab5. J. Cell Sci. *112*, 3667–3675.

Rocca, A., Lamaze, C., Subtil, A., and Dautry-Varsat, A. (2001). Involvement of the ubiquitin/proteasome system in sorting of the interleukin 2 receptor beta chain to late endocytic compartments. Mol. Biol. Cell *12*, 1293–1301.

Rohn, W.M., Rouille, Y., Waguri, S., and Hoflack, B. (2000). Bi-directional trafficking between the trans-Golgi network and the endosomal/lysosomal system. J. Cell Sci. *113*, 2093–2101.

Setiadi, H., Sedgewick, G., Erlandsen, S.L., and McEver, R.P. (1998). Interactions of the cytoplasmic domain of P-selectin with clathrin-coated pits enhance leukocyte adhesion under flow. J. Cell Biol. *142*, 859–871.

Sharma, D.K., Choudhury, A., Singh, R.D., Wheatley, C.L., Marks, D.L., and Pagano, R.E. (2003). Glycosphingolipids internalized via caveolar-related endocytosis rapidly merge with the clathrin pathway in early endosomes and form microdomains for recycling. J. Biol. Chem. *278*, 7564–7572.

Sharma, M., Benharouga, M., Hu, W., and Lukacs, G.L. (2001). Conformational and temperature-sensitive stability defects of the delta F508 cystic fibrosis transmembrane conductance regulator in post-endoplasmic reticulum compartments. J. Biol. Chem. *276*, 8942–8950.

Sheff, D., Pelletier, L., O'Connell, C.B., Warren, G., and Mellman, I. (2002). Transferrin receptor recycling in the absence of perinuclear recycling endosomes. J. Cell Biol. *156*, 797–804.

Sheff, D.R., Daro, E.A., Hull, M., and Mellman, I. (1999). The receptor recycling pathway contains two distinct populations of early endosomes with different sorting functions. J. Cell Biol. *145*, 123–139.

Simonsen, A., Lippe, R., Christoforidis, S., Gaullier, J.M., Brech, A., Callaghan, J., Toh, B.H., Murphy, C., Zerial, M., and Stenmark, H. (1998). EEA1 links PI(3)K function to Rab5 regulation of endosome fusion. Nature *394*, 494–498.

Sonnichsen, B., De Renzis, S., Nielsen, E., Rietdorf, J., and Zerial, M. (2000). Distinct membrane domains on endosomes in the recycling pathway visualized by multicolor imaging of Rab4, Rab5, and Rab11. J. Cell Biol. *149*, 901–914.

Stenmark, H., Parton, R.G., Steele-Mortimer, O., Lutcke, A., Gruenberg, J., and Zerial, M. (1994). Inhibition of rab5 GTPase activity stimulates membrane fusion in endocytosis. EMBO J. *13*, 1287–1296.

Swiatecka-Urban, A., Duhaime, M., Coutermarsh, B., Karlson, K.H., Collawn, J., Milewski, M., Cutting, G.R., Guggino, W.B., Langford, G., and Stanton, B.A. (2002). PDZ domain interaction controls the endocytic recycling of the cystic fibrosis transmembrane conductance regulator. J. Biol. Chem. *277*, 40099–40105.

Ullrich, O., Reinsch, S., Urbe, S., Zerial, M., and Parton, R.G. (1996). Rab11 regulates recycling through the pericentriolar recycling endosome. J. Cell Biol. *135*, 913–924.

van der Sluijs, P., Hull, M., Webster, P., Male, P., Goud, B., and Mellman, I. (1992). The small GTP-binding protein rab4 controls an early sorting event on the endocytic pathway. Cell *70*, 729–740.

van Kerkhof, P., Alves dos Santos, C.M., Sachse, M., Klumperman, J., Bu, G., and Strous, G.J. (2001). Proteasome inhibitors block a late step in lysosomal transport of selected membrane but not soluble proteins. Mol. Biol. Cell *12*, 2556–2566.

Vollenweider, P., Martin, S.S., Haruta, T., Morris, A.J., Nelson, J.G., Cormont, M., Le Marchand-Brustel, Y., Rose, D.W., and Olefsky, J.M. (1997). The small guanosine triphosphate-binding protein Rab4 is involved in insulin-induced GLUT4 translocation and actin filament rearrangement in 3T3–L1 cells. Endocrinology *138*, 4941–4949.

Ward, C.L., Omura, S., and Kopito, R.R. (1995). Degradation of CFTR by the ubiquitin-proteasome pathway. Cell *83*, 121–127.

Weixel, K.M., and Bradbury, N.A. (2001). Mu 2 binding directs the cystic fibrosis transmembrane conductance regulator to the clathrin-mediated endocytic pathway. J. Biol. Chem. *276*, 46251–46259.

Yamashiro, D.J., Tycko, B., Fluss, S.R., and Maxfield, F.R. (1984). Segregation of transferrin to a mildly acidic (pH 6.5) para-Golgi compartment in the recycling pathway. Cell *37*, 789–800.

Yoo, J.S., Moyer, B.D., Bannykh, S., Yoo, H.M., Riordan, J.R., and Balch, W.E. (2002). Non-conventional trafficking of the cystic fibrosis transmembrane conductance regulator through the early secretory pathway. J. Biol. Chem. *277*, 11401–11409.

Yu, A., and Malek, T.R. (2001). The proteasome regulates receptor-mediated endocytosis of interleukin-2. J. Biol. Chem. *276*, 381–385.

Zerial, M., and McBride, H. (2001). Rab proteins as membrane organizers. Nat. Rev. Mol. Cell. Biol. *2*, 107–117.